J. Fluid Mech. (1971), *vol.* 50, *part* 2, *pp.* 335–353
Printed in Great Britain

Slender-body analysis of the motion and stability of a vortex filament containing an axial flow

By SHEILA E. WIDNALL AND DONALD B. BLISS

Department of Aeronautics and Astronautics
Massachusetts Institute of Technology
Cambridge, Massachusetts

(Received 25 April 1971)

Previous results concerning the effects of axial velocity on the motion of vortex filaments are reviewed. These results suggest that a slender-body force balance between the Kutta–Joukowski lift on the vortex cross-section and the momentum flux within the curved filament will give some insight into the behaviour of the filament. These simple ideas are exploited for both a single vortex filament and a vortex pair, both containing axial flow. The stability of a straight vortex filament containing an axial flow to long wave sinusoidal displacements of its centre-line is investigated and the stability boundary obtained. The effect of axial flow on the stability of a vortex pair is explored. It is shown that to lowest order (in the ratio of vortex core radius to distance between the vortices) the effect of axial flow is to reduce the self-induced rotation of a single filament and that this effect can be considered as a change in effective core radius. To the next order, travelling waves appear in the instability, the instability mode for the vortex pair becomes non-planar but the amplification rate of the instability is not affected.

1. Introduction

Recent concern over the hazard presented by the trailing vortex system produced by large subsonic jet aircraft has stimulated interest in tip vortex flow fields and their resulting motion, stability and persistence. One of the most striking features of the tip vortex flow, as observed in flight tests by marking the trailing vortex of an aircraft with smoke from a stationary tower, is a strong axial flow within the vortex core. (In most cases, this flow seems to be directed towards the aircraft.) More generally, vortex flows with axial velocities are a familiar occurrence in many aeronautical and geophysical situations. It is therefore of interest to examine the effects of axial velocities upon the motion and stability of a vortex filament.

The purpose of this paper is to demonstrate that some rather simple ideas of force and momentum flux – in the spirit of slender-body theory – can provide an understanding of the effects of axial flow upon the dynamics of a vortex filament of small cross-section; small in the context of slender-body theory means, of course, small by comparison to the local radius of curvature of the filament or to the wavelength of the perturbation. The results obtained agree with more complex

and complete theories and are expected to be of general usefulness in studies of vortex motion.

The restriction to long waves suggests that the phenomena of vortex breakdown is outside the range of the present model. The stability of a vortex to short wavelength perturbations would have to be analyzed (probably numerically) for each particular distribution of axial and swirl velocities within the core. Such a calculation for a particular vortex containing axial flow was presented by Bergman (1969). (These results will be discussed in §2.)

The motion of a vortex filament without axial flow has been of fundamental interest since the nineteenth century. Kelvin determined the self-induced motion of both a vortex ring and an initially straight sinusoidally perturbed vortex filament assuming a core of uniform vorticity. The radius of the core a is required to be small by comparison to the radius R (ring) or the wavelength λ (sinusoid). More recently, Saffman (1970) presented the general result for the self-induced velocity of a vortex ring with an arbitrary distribution of vorticity within the core (again $a/R \ll 1$) based on an energy theorem.

For the study of the stability of the vortex pair, such as in an aircraft wake, the solution presented by Kelvin for the self-induced motion of a vortex filament of uniform vorticity subjected to a sinusoidal displacement of its centre-line is of fundamental importance. He showed that this filament would rotate without a change of shape about its unperturbed position with an angular velocity given by (Thomson 1910*a*, *b*)

$$\Omega_0 = (\Gamma/4\pi)\, k^2[-\ln(ka) + \tfrac{1}{4} + \ln 2 - \gamma], \tag{1.1}$$

where Γ is the circulation, k the perturbation wave-number and γ is Euler's constant.

The analysis of the stability of a pair of vortex filaments was presented by Crow (1970). He considered the mutual interaction of a pair of such sinusoidally perturbed vortex filaments separated by a distance b. To the self-induced motion given by (1.1) was added the velocity induced at the vortex by the presence and deformation of the other vortex. (Details of this calculation will be discussed in §3.) For a range of wavelengths, the resulting motion of the filaments is an exponential divergence occurring on two tipped planes at an angle of about 45°. The most unstable wavelength is $\lambda = 8{\cdot}4b$ for a vortex core radius $a = 0{\cdot}1b$, a typical value for aircraft. The general features of the basic vortex pair instability are sketched in figure 1.

Since to lowest order (in ka and a/b) the induced velocity of one vortex upon the other is insensitive to the presence of axial flow within the vortex core, the effect of axial flow upon the stability of a vortex pair is found by examining the self-induced motion of a perturbed vortex filament containing axial flow.

Recently Widnall, Bliss & Zalay (1970) presented an analysis (hereafter referred to as I) of the effects of axial flow upon the self-induced motion of a sinusoidally perturbed vortex filament. Results were also presented for the propagation velocity of a vortex ring containing an axial flow – a most unlikely but interesting situation. In this analysis the method of matched asymptotic expansions was used to obtain a general result for the self-induced motion (and the other flow quantities) of a vortex filament with an arbitrary distribution of axial

and swirl velocities. The perturbation analysis required $ka \ll 1$ and w/v at most $O(1)$ where w is axial velocity and v is swirl velocity.

The result obtained in I for the propagation velocity of a vortex ring without axial flow is identical to the result presented by Saffman (1970). The velocity is

$$U_0 = \frac{\Gamma}{4\pi R}\left[\ln\frac{8R}{a} + A - \tfrac{1}{2}\right], \tag{1.2}$$

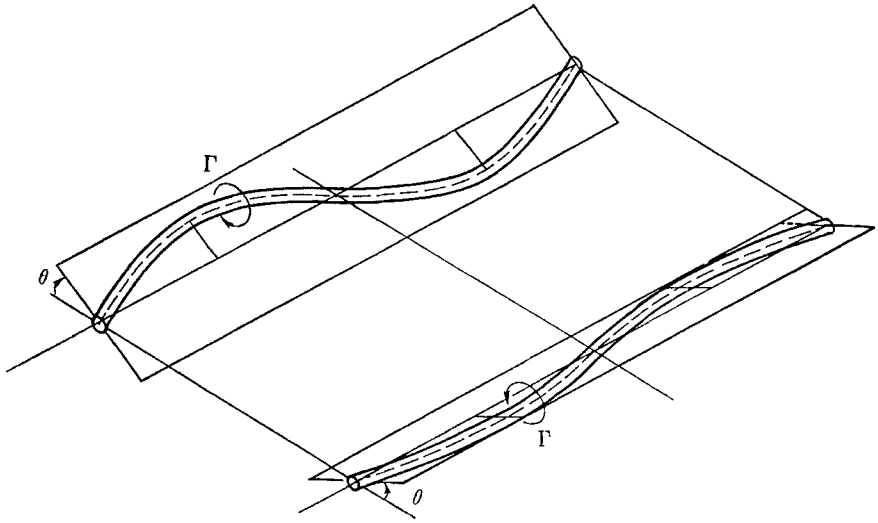

FIGURE 1. General features of the vortex pair instability. The particular instability mode sketched is the symmetric mode.

where the constant A depends only upon the details of the vorticity distribution; e.g. if the vorticity is uniform $A = \frac{1}{4}$. The constant A is defined by the expression

$$\lim_{r\to\infty} 2\pi\int_0^r \tfrac{1}{2}v^2 r\,dr = \frac{\Gamma^2}{4\pi}\left[\ln\frac{r}{a} + A\right], \tag{1.3}$$

where r is a local cylindrical radius at the vortex filament. A is related to the kinetic energy of the vortex. The total kinetic energy of a vortex is infinite; A is finite.

When the effects of axial velocity are included in the analysis (I) it is still possible to obtain the solution analytically. The expression for the velocity of the vortex ring containing axial flow is

$$U = U_0 - \int_0^\infty 2\pi r w^2\,dr \Big/ R\Gamma. \tag{1.4}$$

This result has a very simple physical interpretation. To contain the momentum flux (the integral) within the vortex core, an inward force, acting upon the filament, of magnitude

$$F = -\int_0^\infty 2\pi r w^2\,dr \Big/ R \tag{1.5}$$

is required. This force is provided by a Kutta–Joukowski lift acting upon the

vortex cross-section whenever the velocity of the ring differs from the equilibrium U_0. The lift on the filament is $\Gamma(U-U_0)$. (1.6)

A combination of (1.5) and (1.6) confirms that the ring slows down to provide the lift force necessary to contain the internal flow. (This result, of course, has limitations: it is unlikely that the ring would ever reverse its direction, and it is also obvious that the ring would be unable to contain the axial flow as the flow velocity becomes large. The ring would probably become unstable.)

This simple force/momentum flux balance confirms the result of (1.4) obtained in I by a rather lengthy analysis (and a fortuitous solution, by inspection, of the perturbed vorticity equations). This suggests that an understanding of the motion and stability of vortex filaments containing axial flow may be obtained by an application of some rather simple ideas of lift on a vortex cross-section and momentum flux in a perturbed cylindrical duct by means of slender-body theory, which is valid for $ka \ll 1$, an approximation already inherent in most treatments of vortex filaments.

In the analysis (I) of the effects of axial flow upon the self-induced motion of a perturbed sinusoidal filament a similar result was obtained. The presence of axial flow slows down the rotation by the amount which provides the necessary lift on the vortex filament to turn the internal axial flow. This problem is, however, more complex in that the presence of axial flow within a *rotating* sinusoidal filament requires a balancing Coriolis force which induces travelling waves upon the filament to provide the necessary lift force. The role of the travelling waves in the *diverging* vortex pair instability is not obvious; in fact the sorting out of the effects of rotation and axial flow was the motivation for the development of the slender-body theory.

Another motivation was the interest in the stability of the vortex as the axial velocity becomes very large, i.e. as the vortex becomes a jet. The stability of a jet was studied by Batchelor & Gill (1962). Their results indicate that the sinuous mode ($n = \pm 1$) is always unstable for sufficiently long waves. The long wave jet-vortex model should reduce to the jet as the swirl velocity goes to zero.

The previous analysis (I) was formulated for the case that the axial velocity was – at most – as large as the swirl velocity (as in the aircraft wake). Under these conditions, the unsteady effects which play an essential role in the jet instability are negligible. The slender-body theory allows these effects to be considered and the time scales identified for inclusion in a more complete perturbation analysis.

The present analysis will consider both the self-induced motion of a single vortex filament and the coupled motion of a perturbed vortex pair.

2. Analysis of a single vortex filament

We consider a general sinusoidal perturbation of the vortex filament (as sketched in figure 2) of the form

$$\mathbf{r}(z) = x(z)\mathbf{i} + y(z)\mathbf{j} = x_0 e^{i(kz+\omega t)}\mathbf{i} + y_0 e^{i(kz+\omega t)}\mathbf{j}, \tag{2.1}$$

where the amplitude coefficients x_0 and y_0 are assumed to be small. The vortex filament contains an axial flow w. For convenience, we will take w as constant

across the vortex core although we will indicate how results are obtained for a general distribution.

To obtain the effect of axial flow upon the motion and stability of this vortex filament we apply a slender-body force balance in each x, y plane. The vortex filament is treated as a deformed cylindrical shell containing an internal flow. The total force on the cylindrical cross-section is taken as the Kutta–Joukowski lift produced whenever the motion of the filament differs from the self-induced

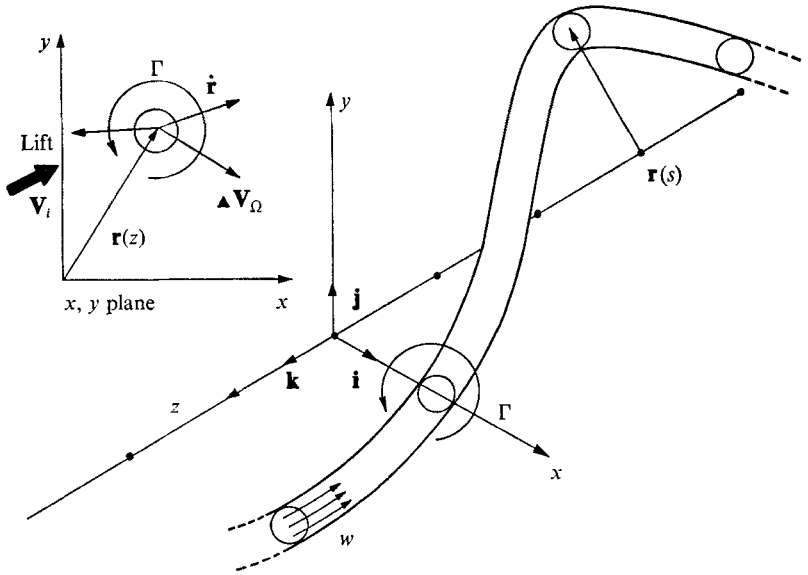

FIGURE 2. Slender vortex filament containing an axial flow.

motion of a vortex filament without axial flow, which, in the limit $ka \to 0$, can support no lift. The remaining terms in the force-momentum balance are due to the hydrodynamic mass of both the external and internal fluids – this is a matter of taste since these terms could as well be considered forces. Beyond its role in the generation of lift, the external fluid may be replaced by an equivalent hydrodynamic mass πa^2. (See appendix A for a detailed discussion of the use of hydrodynamic mass in a flow with circulation.) The hydrodynamic mass of the internal fluid is also πa^2; the effect of axial flow enters through the expression for the absolute acceleration of the internal fluid.

For a given wave-number k (real), the force balance results in a pair of coupled homogeneous algebraic equations for the coefficients x_0 and y_0; the equations also contain the eigenvalue ω. Instability occurs whenever ω has a negative imaginary part. An eigenmode $x_0 \propto y_0$ is a planar sinusoid. The mode $x_0 = \pm i y_0$ is a helix of counter-clockwise or clockwise sense.

We now present the details of the slender-body force balance for the single vortex filament sketched in figure 2. The position of the vortex cross-section in an x, y plane is $\mathbf{r}(z)$, given by (2.1), as indicated in the insert sketch. The velocity of the cross-section is

$$\dot{\mathbf{r}}(z) = i\omega \mathbf{r}(z). \tag{2.2}$$

Since the general deformation is made up of elementary sinusoidal displacements, to lowest order in the amplitude the filament will rotate about the x axis with angular velocity Ω_0, see (1.1), if there is no axial flow within the core; this can also be verified by a detailed integration of the Biot–Savart law taking proper account of the finite vortex core. (If the vorticity within the core is not uniform, the $\frac{1}{4}$ in (1.1) is replaced by the constant A as defined by (1.3).)

The lift force on the vortex cross-section is

$$\mathbf{L} = \Gamma \mathbf{k} \times [\dot{\mathbf{r}} - \mathbf{V}_\Omega], \tag{2.3}$$

where $\mathbf{V}_\Omega = -\Omega_0[y\mathbf{i} - x\mathbf{j}]$, a rigid rotation at an angular velocity Ω_0, see (1.1). Thus if the velocity of the vortex $\dot{\mathbf{r}}$ equals $\mathbf{V}_\Omega$, no lift is produced.

The time derivative of the momentum in the external fluid M_e replaced by its equivalent hydrodynamic mass πa^2 is

$$dM_e/dt = \pi a^2 d^2\mathbf{r}/dt^2. \tag{2.4}$$

The equivalent expression for the internal fluid contains the substantial derivative to account for the acceleration of the moving fluid.

$$dM_i/dt = \pi a^2 D^2 r/Dt^2, \tag{2.5}$$

where $$D/Dt = \partial/\partial t + w\,\partial/\partial x.$$

(If the velocity within the core is not uniform, the slender-body analysis should still be valid if the momentum flux $\pi a^2 w^2$ is replaced by

$$\int_0^\infty 2\pi r w^2\, dr$$

and the mass flux $\pi a^2 w$ is replaced by

$$\int_0^\infty 2\pi r w\, dr.$$

Such a calculation appears in appendix B.)

Equating the lift force (2.3) to the sum of (2.4) and (2.5), we obtain

$$\frac{d^2 r}{dt^2} + \frac{D^2 r}{Dt^2} = \frac{\Gamma}{\pi a^2}\mathbf{k} \times [\dot{\mathbf{r}} - \mathbf{V}_\Omega]. \tag{2.6}$$

If the vorticity is uniform, $\Gamma/2\pi a^2$ equals Ω, the angular velocity of the vortex core. (Both Γ and Ω will be taken as positive as sketched in figure 2.) In any case, we will use Ω to non-dimensionalize ω and kw, introducing

$$\sigma = \omega/\Omega \quad \text{and} \quad S = kw/\Omega. \tag{2.7), (2.8}$$

For convenience in obtaining the eigenvalues and eigenmodes, the final equations for x_0 and y_0 are expressed in matrix notation

$$[C]\begin{Bmatrix} x_0 \\ y_0 \end{Bmatrix} = 0. \tag{2.9}$$

The matrix C, obtained from (2.6) and the definitions (2.7) and (2.8), is

$$[C] = \begin{bmatrix} \sigma^2 + \sigma S + \frac{1}{2}S^2 - \frac{1}{2}(ka)^2 K & -i\sigma \\ i\sigma & \sigma^2 + \sigma S + \frac{1}{2}S^2 - \frac{1}{2}(ka)^2 K \end{bmatrix}, \tag{2.10}$$

where $$K = -2\Omega_0/\Omega(ak)^2 = [-\ln(ka) + A + \ln 2 - \gamma].$$

The eigenvalues are found by setting the determinant of C equal to zero. The eigenmodes are then determined by solving either of the two equations in (2.9). The determinant of C gives a quartic for σ. However, it can be seen by inspection that the eigenmodes are $x_0 = \pm iy_0$ and that the quartic can be factored.

$$[\sigma^2 + \sigma S + \tfrac{1}{2}S^2 - \tfrac{1}{2}(ka)^2K - \sigma][\sigma^2 + \sigma S + \tfrac{1}{2}S^2 - \tfrac{1}{2}(ka)^2K + \sigma] = 0. \quad (2.11)$$

For $x = iy_0$ (a helix of counterclockwise sense) the eigenvalue σ_+ is

$$\sigma_+ = -\tfrac{1}{2}(S-1) - \tfrac{1}{2}(1 - 2S - S^2 + 2(ka)^2K)^{\frac{1}{2}}; \quad (2.12)$$

the root of the quadratic is chosen so that at $S = 0$

$$\sigma_+ = \omega/\Omega = \Omega_0/\Omega. \quad (2.13)$$

This modes becomes unstable for

$$S > \{2(1 + (ka)^2K)\}^{\frac{1}{2}} - 1 \approx 2^{\frac{1}{2}} - 1 + 2^{-\frac{1}{2}}(ka)^2K \quad (2.14)$$

or, since $ka \ll 1$, for $S < 2^{\frac{1}{2}} - 1$. For $x_0 = -iy_0$ (a helix of clockwise sense), the eigenvalue σ_- is

$$\sigma_- = -\tfrac{1}{2}(S+1) + \tfrac{1}{2}(1 + 2S - S^2 + 2(ka)^2K)^{\frac{1}{2}}. \quad (2.15)$$

This mode becomes unstable for

$$S > \{2(1 + (ka)^2K)\}^{\frac{1}{2}} + 1 \quad (2.16)$$

or approximately $S > 2^{\frac{1}{2}} + 1$, a larger value of S than for the $x_0 = iy_0$ mode.

The parameter S, see (2.8), which determines the stability for a vortex containing an axial flow may be rewritten using $\Omega = v/a$ where v is the swirl velocity at the core radius a if the vorticity is uniform, otherwise v is a typical swirl velocity. Instability occurs whenever

$$(ka)w/v > 2^{\frac{1}{2}} - 1. \quad (2.17)$$

Since the slender-body analysis is restricted to $ka \ll 1$, the instability of a single vortex containing an axial flow in the limit $ka \gg 1$ occurs for $w \gg v$. This instability is not likely to be important in the tip vortex flow field where the axial velocities are of the same order as the swirl velocities, but it may occur in other vortex flow situations. As the swirl goes to zero, the vortex with axial flow becomes a jet. In this limit ($\Omega \to 0$, $S \to \infty$) the eigenvalues become

$$\sigma = \omega/\Omega = -(kw/2\Omega) \pm \tfrac{1}{2}i(kw/\Omega) \quad (2.18)$$

or

$$\omega = -\tfrac{1}{2}kw \pm \tfrac{1}{2}i(kw).$$

This result agrees with that given by Batchelor & Gill (1962) for a jet with uniform axial velocity w as $ka \to 0$; the wave speed of the jet instability is $\frac{1}{2}w$, the amplification rate ω_i is $\frac{1}{2}kw$.

For $ka \sim O(1)$, the stability analysis of vortex containing an axial flow would have to be carried out for each particular distribution of axial and swirl velocities. Bergman (1969) reported such a calculation for a meteorogically interesting vortex. Although he anticipated that his numerical results would show stability as the axial flow diminished, in fact this did not occur. In appendix B we calculate the long wave stability boundary for the particular mass and momentum flux

distributions in his vortex. The axial velocity and circulations distributions for this particular vortex are shown in figure 3 (along with a simple function which we shall use to approximate the circulation distribution).

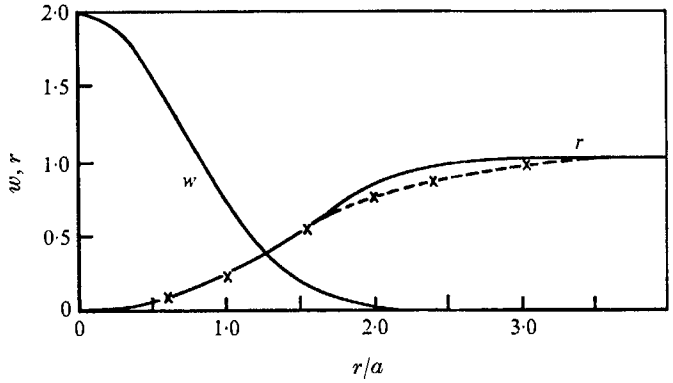

FIGURE 3. Initial axial velocity and circulation distribution in Bergman's stability calculation. × - - - ×, exponential fit to circulation profile.

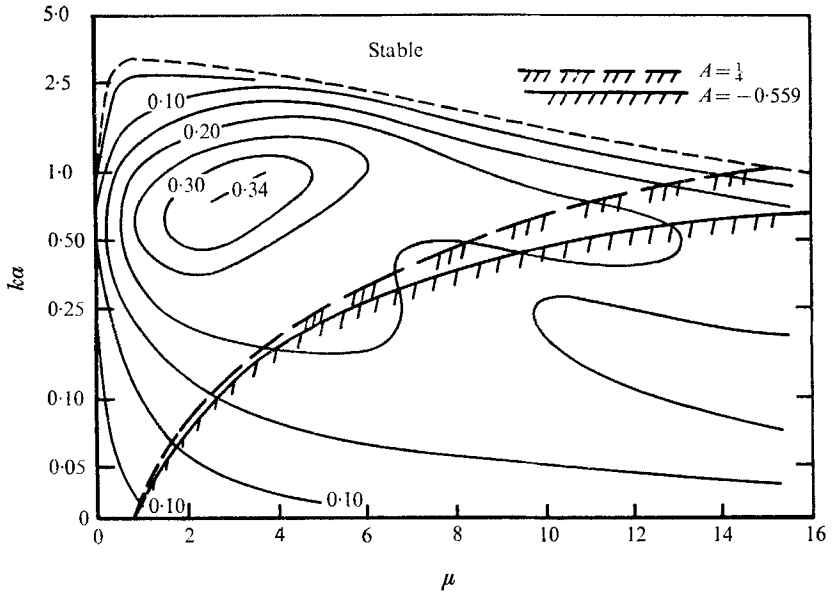

FIGURE 4. Contours of constant amplification rate λ_i (from Bergman 1969) for the helical mode of a single vortex containing an axial flow as a function of wave-number and swirl parameter, $\mu = \Gamma/aw$, where $\lambda_i = \mathrm{Im}\{\sigma\}\mu/2\pi$. Cross-hatch curves show the long wave stability boundary, $\lambda_i = \mathrm{Im}\{\sigma\} = 0$, for two different vorticity distributions.

Figure 4, taken from Bergman's paper, shows contours of constant amplification rate λ_i as a function of ka and μ; the parameter μ is proportional to ka/S;

$$\lambda_i = \mathrm{Im}\{\sigma\}\mu/2\pi$$

(see appendix B). The slender-body stability boundary (B 7) is

$$\mu = 8\pi ka/\{1 + 2(ka)^2 K\},$$

where $K \simeq [-\ln(ka) - 0{\cdot}39]$ for the particular vorticity distribution; this is superimposed upon his results in figure 4. Below this boundary the flow should be stable; the reason for the discrepancy is not known. The analytic form of the long wave stability boundary may be useful in future numerical investigations of vortex stability. If both the upper (short wave) and lower (long wave) stability boundaries are correct, a rather complete picture of the stability of a vortex containing an axial flow to sinusoidal displacements of its centre-line is obtained.

In a parallel investigation, Moore & Saffman (1971) formulated the linearized perturbation problem for waves of amplitude smaller than the core size on a vortex of uniform vorticity containing a uniform axial flow. In this case the resulting equations for both the internal and external fluid are (different) forms of Bessel's equation. In the long wavelength limit the stability boundary is essentially that predicted by the slender-body model (2.14), (2.16).

It is of some interest to combine the two eigenmodes (if both are stable) to form a planar sinusoidal mode. In the general case the planar sinusoidal wave will travel as well as rotate.

The eigenmodes can be written

$$\left.\begin{aligned} \mathbf{r}_+ &= [i\mathbf{i}+\mathbf{j}]e^{i(kz+\sigma_+\Omega t)} \\ \text{and} \qquad \mathbf{r}_- &= [-i\mathbf{i}+\mathbf{j}]e^{i(kz+\sigma_-\Omega t)}. \end{aligned}\right\} \tag{2.19}$$

These results were derived with the implicit assumption that the wave-number k was positive. For negative k (and therefore negative S)

$$\left.\begin{aligned} \sigma_+(-S) &= -\sigma_+(|S|) \\ \text{and} \qquad \sigma_-(-S) &= -\sigma_+(|S|). \end{aligned}\right\} \tag{2.20}$$

The eigenmodes become

$$\left.\begin{aligned} \mathbf{r}_- &= [i\mathbf{i}+\mathbf{j}]e^{-i|k|z-i\sigma_-\Omega t}, \\ \mathbf{r}_+ &= [-i\mathbf{i}+\mathbf{j}]e^{-i|k|z-i\sigma_+\Omega t}. \end{aligned}\right\} \tag{2.21}$$

The general form of a planar travelling rotating sinusoidal mode is

$$\mathbf{r} = e^{i\sigma_r\Omega t}[i\mathbf{i}+\mathbf{j}]\,[e^{i(ks+\sigma_t\Omega t)} + e^{-i(ks+\sigma_t\Omega t)}], \tag{2.22}$$

where σ_r is the rotational frequency (the mode rotates counterclockwise if σ_r is positive) and $-\sigma_t\Omega/k$ is the phase speed of the travelling wave. It can be seen by inspection that this mode is the sum of $\mathbf{r}_+$ from (2.19) and $\mathbf{r}_-$ from (2.21). The rotational and translational frequencies σ_r and σ_t are given by

$$\left.\begin{aligned} \sigma_t+\sigma_r = \sigma_+, \quad \sigma_t-\sigma_r = \sigma_- \\ \text{or} \qquad \sigma_t = \tfrac{1}{2}(\sigma_++\sigma_-), \quad \sigma_r = \tfrac{1}{2}(\sigma_+-\sigma_-). \end{aligned}\right\} \tag{2.23}$$

The rotational frequency of the planar mode then becomes

$$\sigma_r = \tfrac{1}{2} - \tfrac{1}{4}(1-2S-S^2+2(ka)^2k)^{\frac{1}{2}} - \tfrac{1}{4}(1+2S-S^2+2(ka)^2k)^{\frac{1}{2}}. \tag{2.24}$$

For small S, the rotational frequency is

$$\sigma_r \approx -\tfrac{1}{2}[(ka)^2K - S^2]. \tag{2.25}$$

This result agrees with the analysis of I; the effect of axial velocity is to slow the rotation of the planar sinusoid. The phase speed of travelling waves along the filament for small S is

$$c = -\sigma_t \Omega/k \approx \tfrac{1}{4} w S^2 = \tfrac{1}{4} w(ka)^2 \, [w/v]^2. \tag{2.26}$$

When the axial and swirl velocities are of the same order, as in an aircraft wake, the travelling wave speed is very small being $O(w(ka)^2)$; the lift producing capability of the filament suppresses travelling waves.

3. The vortex pair instability

The coupled pair instability is shown in figure 1. In the absence of axial flow, the instability mode of each vortex is planar; the amplitude grows exponentially in time (Crow 1970). Working in a co-ordinate system fixed with the descending pair, we will take the more general form (2.1) for the assumed perturbation of the vortex which allows for the possibility of both travelling waves and non-planar deformations.

The required modification to the force balance of § 2 for a pair of vortex filaments is to include the forces induced by the presence and deformation of the other vortex. Both the velocity and pressure fields due to the other vortex induce forces on the vortex cross-section. Of these, the most important is the Kutta–Joukowski lift force, the product of circulation and the induced velocity due to the other vortex. (This, of course, is largely balanced by the lift due to the resulting motion of the vortex.) The net force on the vortex cross-section due to the pressure field is caused primarily by the unsteadiness of the induced velocity field as the instability proceeds. This term makes only a small change in the stability boundary of the jet-vortex, as will be seen.

The deformations of the two vortices are

$$\mathbf{r} = x_0 e^{i(kz+\omega t)} \mathbf{i} + y_0 e^{i(kz+\omega t)} \mathbf{j} \tag{3.1}$$

for the vortex in question, and

$$\mathbf{r} = x_1 e^{i(kz+\omega t)} \mathbf{i} + y_1 e^{i(kz+\omega t)} \mathbf{j} \tag{3.2}$$

for the other vortex. The general instability can be represented as a combination of modes, the symmetric ($x_1 = -x_0, y_1 = y_0$) and the antisymmetric ($x_1 = x_0$, $y_1 = -y_0$). To first order in the amplitude of the deformation, the induced velocity $\mathbf{v}_i$ at the position of the vortex $\mathbf{r}$ due to the other vortex is the sum of $\mathbf{v}_0$, the velocity at the perturbed position of the vortex due to the other vortex in its unperturbed position and $\mathbf{v}_1$, the induced velocity due to the deformation of the other vortex. In the neighbourhood of the vortex cross-section $\mathbf{v}_0$ is a local steady but non-uniform flow given by

$$\mathbf{v}_0 = (\Gamma/2\pi b^2) \, [y_0 \mathbf{i} + x_0 \mathbf{j}] e^{i(kz+\omega t)}, \tag{3.3}$$

a local two-dimensional potential 'corner flow', a flow with uniform strain. In the neighbourhood of the vortex cross-section, $\mathbf{v}_1$ is a local free stream of magnitude

$$\mathbf{v}_1 = \frac{\Gamma}{2\pi b^2} [y_1[-(kb)^2 K_0(kb) - (kb) K_1] \mathbf{i} - x_1[(kb) K_1(kb)] \mathbf{j}] \, e^{i(kz+\omega t)}, \tag{3.4}$$

where K_1 and K_0 are modified Bessel functions of the second kind; y_1 and x_1 are the amplitude coefficients of the deformation of the other vortex (3.2). If the amplitude of the deformation grows, $\mathbf{v}_1$ is an accelerating free stream. The derivations of (3.3) and (3.4) appear in the analysis of Crow (1970). The total induced velocity $\mathbf{v}_1$ is then written

$$\mathbf{v}_1 = \frac{\Gamma}{2\pi b^2}[[1 \mp Y]y_0\mathbf{i} + [1 \pm X]x_0\mathbf{j}]e^{i(kz+\omega t)}, \tag{3.5}$$

where the notation

$$X = (kb)^2K_1, \quad Y = (kb)^2K_0 + (kb)K_1$$

has been introduced. The upper sign is taken for the symmetric mode, the lower sign for the antisymmetric mode.

The forces induced by the presence and deformation of the other vortex are now calculated. In appendix A the total force on a cylindrical cross-section with circulation moving through the flow field of (3.3) is shown to be the sum of the Kutta lift, the inertial force due to the hydrodynamic mass and the pressure force required to hold the cylinder in place. Unsteady effects due to moving about in a non-uniform flow cancel.

Of most importance is the lift force acting on the vortex cross-section due to the induced velocity $\mathbf{v}_i$. Referring to the insert sketch in figure 2, we see that if an external velocity field $\mathbf{v}_i$ is added to the flow of the single vortex filament, the total lift force on the vortex cross-section (2.3) becomes

$$\mathbf{L} = \Gamma\mathbf{k} \times (\dot{\mathbf{r}} - \mathbf{v}_\Omega - \mathbf{v}_i]. \tag{3.6}$$

The total flow at the cylinder due to the other vortex consists of the uniform straining flow (3.3) and the accelerating free stream (3.4). The force required to hold the cylinder in place in the uniform straining flow is

$$\mathbf{F} = 2\pi a^2(\Gamma/2\pi b^2)^2[x\mathbf{i} + y\mathbf{j}]. \tag{3.7}$$

The force on the cylinder in the accelerating stream is

$$\mathbf{F} = 2\pi a^2 d\mathbf{v}_1/dt. \tag{3.8}$$

The total force on the vortex cross-section – beyond effects due to hydrodynamic mass – is the sum of (3.6), (3.7) and (3.8).

$$\mathbf{F} = 2\pi a^2\Omega\mathbf{k} \times [\dot{\mathbf{r}} - \mathbf{v}_\Omega - \mathbf{v}_i] + 2\pi a^2\omega i\mathbf{v}_1 + 2\pi a^2[\Omega(a/b)^2]^2\mathbf{r}, \tag{3.9}$$

where Γ has been replaced by $2\pi a^2\Omega$.

The first term in (3.9) dominates; the second term, of higher order by a^2/b^2, is of minor importance; the last term, $O((a/b)^4)$, is negligible and will not be included in the analysis. The total force (3.9) is equated to the time derivative of fluid momentum in and near the single filament, the sum of (2.4) and (2.5). The form of the stability problem for the vortex pair is the same as for a single filament (2.9) with the additional force terms now included in the matrix C. For the coupled vortex pair instability, C becomes

$$[C] = \begin{bmatrix} A - \sigma^2 - \sigma S - (a/b)^2[1 \pm X] & i\sigma[1 \pm (a/b)^2 Y] \\ -i\sigma[1 \pm (a/b)^2 X] & A - \sigma^2 - \sigma S + (a/b)^2[1 \mp Y] \end{bmatrix}, \tag{3.10}$$

where $A = \frac{1}{2}\{(ka)^2K - S^2\}$ (recall that plus is taken for the symmetric, minus for the antisymmetric mode). For the single vortex case $b \to \infty$, (3.10) reduces to (2.10).

A jet instability would be expected for the vortex pair as the axial velocity becomes very large, $S \sim O(1)$. Under these conditions the time scale σ will be $O(1)$. The presence of the other vortex would affect this instability only slightly, to $O(a^2/b^2)$.

However, for the case that the axial velocities are of the same order as (or smaller than) the swirl velocities, S is $O(ka)$, $(ka) \ll 1$. The appropriate scaling for the eigenvalue σ is then

$$\sigma = \epsilon^2\bar{\sigma}, \tag{3.11}$$

where $\epsilon = a/b$ and $\bar{\sigma}$ is $O(1)$. The eigenvalue problem for $\bar{\sigma}$, obtained from (3.10) is

$$\begin{bmatrix} (kb)^2G - [1 \pm X] - \epsilon\sigma kb\alpha - \epsilon^2\sigma^2 & i\sigma[1 \pm \epsilon^2 Y] \\ -i\sigma[1 \pm \epsilon^2 X] & (kb)^2G + [1 \mp Y] - \epsilon\sigma kb\alpha - \epsilon^2\sigma^2 \end{bmatrix} = 0, \tag{3.12a}$$

where

$$\alpha = w/v = w/\Omega a \quad \text{and} \quad G = [\tfrac{1}{2}(K - \alpha^2)]. \tag{3.12b}$$

To obtain a simple approximate solution, the eigenvalue σ is expanded in a perturbation series

$$\bar{\sigma} = \bar{\sigma}_0 + \epsilon\bar{\sigma}_1 + \epsilon^2\bar{\sigma}_2 \tag{3.13}$$

(this is valid away from multiple roots). When (3.13) is substituted into (3.12), the following equations for σ_0, σ_1 and σ_2 are obtained:

$$\left.\begin{aligned} \bar{\sigma}_0^2 &= -[(1 \pm X) - (kb)^2G][1 \mp Y + (kb)^2G], \\ \bar{\sigma}_1 &= \tfrac{1}{2}kb\alpha[\pm X \mp Y - 2(kb)^2G], \\ \bar{\sigma}_2 &= (1/2\bar{\sigma}_0)[-\bar{\sigma}_0^2[2(kb)^2G + (kb)^2\alpha] + \bar{\sigma}_1^2]. \end{aligned}\right\} \tag{3.14}$$

The lowest-order term in $\bar{\sigma}(\bar{\sigma}_0)$ is the eigenvalue associated with the aircraft wake stability problem as formulated by Crow for a vortex pair without axial flow and as modified in I to include arbitrary distribution of axial and swirl velocity. When the flow is unstable, σ_0 is purely imaginary; the instability is a simple divergence. To lowest order, the eigenmode is

$$x_0 = \frac{|\sigma_0|}{[1 \pm X - (kb)^2G]}\, y_0, \tag{3.15}$$

a planar mode.

In I, it was shown that the results obtained by Crow (1970) for the stability of a vortex pair with uniform vorticity in the core can be used for an arbitrary distribution of swirl and axial velocity (which affects only G) if an effective core radius

$$a_e = a\,\exp(\tfrac{1}{4} - A + \alpha^2) \tag{3.16}$$

is taken. With this definition, G, from (3.12 b), becomes

$$G = \tfrac{1}{2}[-\ln(ka_e) + \tfrac{1}{4} + \ln 2 - \gamma], \tag{3.17}$$

i.e. the 'G' for a vortex core of radius a_e, with uniform vorticity and no axial flow; a_e then incorporates the effects of axial and swirl velocity distribution. Some general features of this instability are shown in figures 5 and 6. Figure 5 shows the

stability boundaries for the symmetric mode as a function of wavelength λ/b and effective vortex core radius a_e/b; the curve in the centre of the instability region is the most unstable wavelength. Figure 6 shows $\bar{\sigma}_0$ for the most unstable wave as a function of a_e/b.

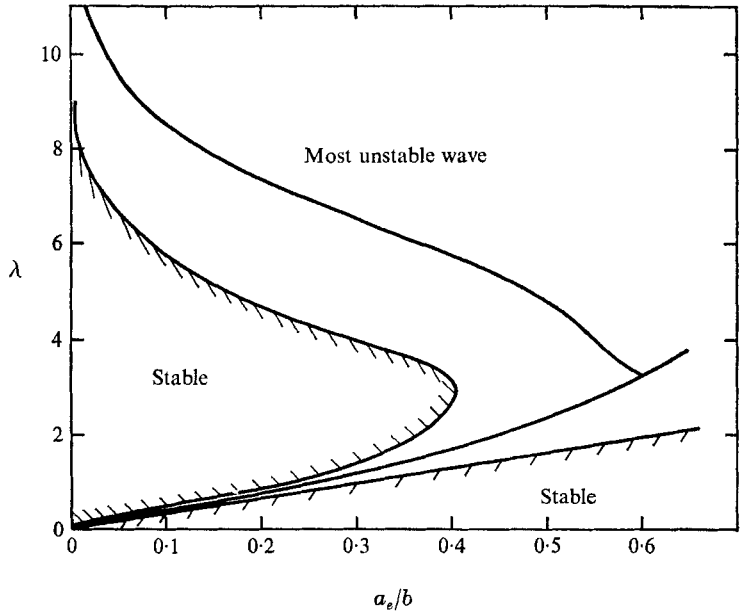

FIGURE 5. Stability diagram for the vortex pair. The cross-hatched lines show the stability boundaries; the solid curve shows the wavelengths of maximum amplification for each a_e/b. The upper curve shows the most unstable long wave, the lower curve the most unstable short wave.

The correction to the eigenvalue $\bar{\sigma}_1$ is always real and for conditions of instability probably always positive (as checked numerically). $\bar{\sigma}_1$ gives no additional contribution to the amplification rate of the instability but introduces travelling waves into the eigenmode. When the self-induced rotation, $(kb)^2 G$, dominates (typically – though not always – when the vortex is stable), the waves travel in the direction of the axial flow; when the vortex is unstable the waves travel in the direction opposed to the axial flow. The physical reason for this is not yet understood.

An expression for the wave speed, $c = -\omega/k$, can be obtained by working back through the non-dimensionalization introduced in (2.7), (3.11), (3.13) to give

$$c = w(a/b)^2[\pm X \mp Y - 2(kb)^2 G]; \tag{3.18}$$

the wave speed is then $O((a/b)^2)$ times the axial velocity w. Another interesting feature of the solution to this order is the eigenmode,

$$x_0 = \frac{-i\bar{\sigma}_0 - i\epsilon\bar{\sigma}_1}{(1 \pm X - (kb)^2 G - \epsilon kb\alpha\sigma_0)} y_0 \tag{3.19}$$

or

$$x_0 = \frac{y_0|\sigma_0|}{[1 \pm k^2 b^2 G]} - \left(\frac{i\epsilon\bar{\sigma}_1}{[1 \pm X - (kb)^2 G]} + \frac{i\sigma_0^2 \epsilon kb\alpha}{[1 \pm X - (kb)^2 G]^2}\right) y_0.$$

The general form is $x_0 = Ay_0 + i\epsilon By_0$; the mode is predominately planar with a small helicity. Seen from on edge it would be slightly elliptical. Thus to the order that travelling waves appear, the mode is no longer planar.

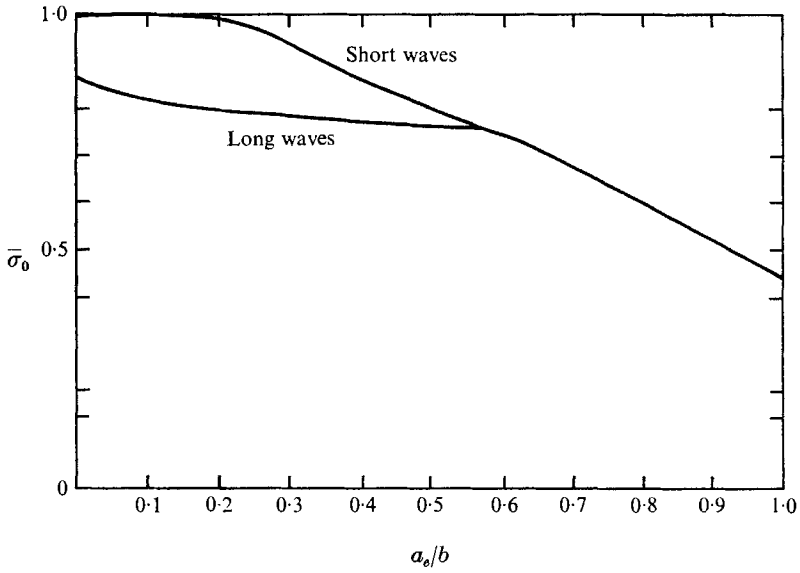

FIGURE 6. Amplification rate of the most unstable wave for the vortex pair instability. Long and short wave branches of this curve give the amplification rates for the long and short wave instability modes from figure 5.

The correction $\bar{\sigma}_2$ is again always imaginary and represents a correction to the amplification rate. Since $\bar{\sigma}_0$ is negative imaginary for conditions of instability $\bar{\sigma}_2$ is always positive in these cases. It therefore represents a reduction of the amplification rate.

When the axial velocity becomes much larger than the swirl velocity, the instability of a vortex pair should differ only slightly from that of a single filament. Since σ is now $O(1)$, the appropriate form of the eigenvalue problem from (3.10) is

$$\begin{vmatrix} A-\sigma^2-\sigma S-\epsilon^2[1\pm X] & i\sigma[1\pm\epsilon^2 Y] \\ -i\sigma[1\pm\epsilon^2 X] & A-\sigma^2-\sigma S+\epsilon^2[1\mp Y] \end{vmatrix} = 0, \tag{3.20}$$

where ϵ is again a/b. For $\epsilon = 0$, the eigenvalues σ are given by (2.12) and (2.13); the stability boundary (2.14) is $S \cong 2^{\frac{1}{2}} - 1 + (ka)^2 K/2^{\frac{1}{2}}$. We will investigate the effect of the other vortex on this stability boundary. Since the stability boundary occurs at a double root $\sigma = \sigma_0 \pm 0$, the perturbation is not as straightforward as the previous case. For this case, we will perturb S as well as σ and find the new stability boundary as a function of ϵ.

Define

$$S = S_0 + \epsilon^2 S_1,$$

where

$$S_0 = 2^{\frac{1}{2}} - 1 + (ka)^2 K/2^{\frac{1}{2}}. \tag{3.21}$$

At $\epsilon = 0$, $S = S_0$; the eigenvalue is

$$\sigma_0 = \tfrac{1}{2}(1 - S_0). \tag{3.22}$$

To $O(\epsilon^2)$, the determinant of (3.20) may be written

$$f_0(\sigma) - \epsilon^2[A_0 - \sigma^2 - S_0\sigma]\,[2\sigma S_1 + 2S_1 S_0 \pm X \mp Y] \pm \epsilon^2[Y - X]\sigma^2 = 0, \tag{3.23}$$

where $f_0(\sigma)$ is the polynomial in σ obtained from (3.23) for $\epsilon = 0$, and

$$A_0 = \tfrac{1}{2}\{(ka)^2 K - S_0^2\},$$

the value of A at $S = S_0$.

At the stability boundary ($\sigma = \sigma_0$) $f_0(\sigma)$ has a double root; therefore near $\sigma = \sigma_0$,

$$f_0(\sigma) \approx (\sigma - \sigma_0)^2\,(\sigma_0 - \sigma_{01})\,(\sigma_0 - \sigma_{02}), \tag{3.24}$$

where σ_{01} and σ_{02} are the *two* roots of the quadratic for the $x_0 = -iy_0$ mode (2.15).

$$\sigma_{01,02} = -\tfrac{1}{2}(S + 1) \pm \tfrac{1}{2}(1 + 2S - S^2 + 2(ka)^2 K)^{\frac{1}{2}}. \tag{3.25}$$

Near the stability boundary, we expand σ as

$$\sigma = \sigma_0 + \epsilon\sigma_1 + \ldots. \tag{3.26}$$

To lowest order, (3.23) becomes

$$\sigma_1^2(\sigma_0 - \sigma_{01})\,(\sigma_0 - \sigma_{02}) - \sigma_0(2\sigma_0 S_1 + 2S_1 S_0 \pm X \mp Y) \pm (Y - X)\sigma_0^2 = 0. \tag{3.27}$$

From (3.27) we obtain

$$\sigma_1 = -2^{-\frac{1}{2}}[-[(S_0 + 1)\,S_1 \mp \tfrac{1}{2}(3 - S_0)\,(Y - X)]]^{\frac{1}{2}}. \tag{3.28}$$

The perturbed stability boundary for the slightly coupled jet-vortex pair is found by setting $\sigma_1 = 0$ and solving for S_1.

$$S_1 = \pm \tfrac{1}{2}(Y - X)\left(\frac{3 - S_0}{S_0 + 1}\right). \tag{3.29}$$

Since $Y - X$ is always positive, the instability occurs at a lower value of S (axial velocity times wave-number) for the symmetric mode and at a higher value of S for the antisymmetric mode. The difference is, however, rather small since the appropriate perturbation (3.21) of the stability boundary is

$$S = S_0 + \epsilon^2 S_1.$$

4. Conclusions

The application of slender-body theory to the motion and stability of a vortex containing an axial flow to long wavelength sinusoidal displacements of its centre-line has provided some new results and an understanding of some results obtained by other methods. The new results are: first, a stability boundary for the long wave perturbations of a vortex with an arbitrary distribution of swirl and axial velocities; second, an ordering – in the small parameter a/b – of the various effects of axial flow on the stability of a vortex pair in both the aircraft-wake and jet-vortex limits. The slender-body theory also identifies the appropriate time

scales for the various instabilities of both a single vortex and a vortex pair; this will allow a more complete perturbation analysis to be done.

The authors wish to thank Philip Saffman for stimulating discussions on many aspects of vortex flows. This work was supported by the Air Force Office of Scientific Research (OSR) under contract F44620-69-C-0090.

Appendix A. Force on a cylinder with circulation moving through a flow with uniform strain

To justify the use of the simple expression (in (2.4)) πa^2 for the hydrodynamic mass of the circular cross-section of the vortex filament, it is necessary to show that the force on a circular cylinder with circulation moving about in an arbitrary (unsteady) manner through a uniform straining flow (which to lowest order represents the effect at the vortex of any non-uniform flow) separates into a pressure force due to position in a non-uniform flow, a lift force due to the product of circulation and velocity and an inertial force, the product of the hydrodynamic mass πa^2 times the acceleration of the cylinder. The particular non-uniform flow at the cross-section due to the presence of the other vortex has a complex potential

$$W(z) = -i\tfrac{1}{2}z^2\Gamma/2\pi b^2. \tag{A 1}$$

We consider a cylinder located at the point z_0 in this flow. We shall work in a local co-ordinate system moving with the cylinder at the velocity $\dot{z}_0$. (For a cylinder, translational motion only need be considered.)

The complex potential of the flow, expressed in the local complex variable ζ, is

$$W(\zeta) = (-i\Gamma/2\pi b^2)\,\tfrac{1}{2}(\zeta+z_0)^2. \tag{A 2}$$

To this is added the apparent free stream due to the motion of the co-ordinate system:

$$W(\zeta) = (-i\Gamma/2\pi b^2)\,\tfrac{1}{2}(\zeta^2+2\zeta z_0+z_0^2) - |\dot{z}_0|e^{-i\alpha}\zeta, \tag{A 3}$$

where $|\dot{z}_0|$ is the magnitude and α is the angle between the velocity vector and the real axis. A cylinder of radius a, fixed with respect to the moving co-ordinates, is inserted by application of the circle theorem (Milne-Thompson 1968). A point vortex may also be added at the centre of the cylinder. The complex potential of a cylinder with circulation in a uniform straining flow is then

$$W(\zeta) = \frac{-i\Gamma}{2\pi b^2}\left\{\frac{1}{2}\left(\zeta^2-\frac{a^4}{\zeta^2}\right)+\left(z_0\zeta-\frac{a^2\bar{z}_0}{\zeta_0}\right)+z_0^2-\bar{z}_0^2\right\} - |\dot{z}_0|\left(\zeta e^{-i\alpha}+\frac{a^2}{\zeta}e^{i\alpha}\right) - i\left(\frac{\Gamma}{2\pi}\right)\log\zeta, \tag{A 4}$$

where $\bar{z}_0$ is the complex conjugate of z_0.

The velocity potential, referred to a fixed frame instantaneously coincident with the moving frame, is

$$\phi_F = \phi_M + \mathrm{Re}\,(|\dot{z}_0|e^{-i\alpha}\zeta), \tag{A 5}$$

where

$$\phi_M = \mathrm{Re}\{W(\zeta)\}.$$

To calculate the pressure on the cylinder we use the pressure equation referred to a moving axis as given by Milne-Thompson (1968),

$$p+\tfrac{1}{2}q_r^2+\partial\phi_F/\partial t-\tfrac{1}{2}|\dot{z}_0|^2 = C(t), \tag{A 6}$$

where q_r is the velocity in the moving frame. (The density has been taken as unity.)

The force is calculated using the extended Blasius theorem (Milne-Thompson 1968)

$$X - iY = -i\oint p\, d\bar{\zeta}. \tag{A 7}$$

Since the complex potential $W(\zeta)$, which enters in both q_r and ϕ_M, is purely real on the cylinder, some of the integrals in (A 7) may be written as analytic functions of the complex variable ζ (or $\bar{\zeta}$), to obtain

$$X - iY = i\frac{1}{2}\oint \left(\frac{dW}{d\zeta}\right)^2 d\zeta + i\frac{\partial}{\partial t}\oint \overline{W} d\bar{\zeta} + i|\dot{z}_0| \oint \mathrm{Re}\{e^{-i\alpha}\zeta\} d\bar{\zeta}. \tag{A 8}$$

This is evaluated by a straightforward application of Cauchy's integral theorem (the last integral is simply evaluated) to give

$$X - iY = 2\pi a^2 \bar{z}_0 \left(\frac{\Gamma}{2\pi b^2}\right)^2 + \frac{\Gamma}{2\pi b^2} z_0 \Gamma - i|\dot{z}_0| e^{-i\alpha}\Gamma - \pi a^2 |\ddot{z}_0| e^{-i\alpha}. \tag{A 9}$$

The various terms in the total force have very simple interpretations. The effects of non-uniformity, circulation and unsteadiness separate. The first term is the force required to hold the cylinder in place in the non-uniform flow, the second is the Kutta–Joukowski lift due to the 'free stream' velocity at the point z_0, the third is the Kutta lift due to any motion of the cylinder, the last is the inertial force due to the hydrodynamic mass πa^2.

One would have expected some cross terms involving a force due to a rate of change of position through a non-uniform flow but in fact these cancel. Since the circulation is taken as independent of time, there is no effect of circulation on the force due to unsteady motion.

Appendix B. Application of the slender-body theory to an atmospheric vortex

The particular vortex flow studied by Bergman (1969) had an axial velocity distribution

$$w(r) = 2\bar{w} e^{-(r/a)^2} \tag{B 1}$$

and a distribution of circulation

$$\frac{\Gamma(r)}{\Gamma_\infty} = \frac{\displaystyle\int_0^{r/a} \exp\left[-\xi^2 + 4\int_0^{\xi} \frac{(1-e^{-\eta^2})}{\eta} d\eta\right] \xi\, d\xi}{\displaystyle\int_0^{\infty} \exp\left[-\xi^2 + \int_0^{\xi} \frac{1-e^{-\eta^2}}{\eta} d\eta\right] \xi\, d\xi}. \tag{B 2}$$

These functions are shown in figure 3. For convenience we approximate the circulation profile as

$$\Gamma/\Gamma_0 = 1 - e^{-(r/1{\cdot}65a)^2}. \tag{B 3}$$

The axial momentum flux within this vortex is

$$M = \int_0^{\infty} 2\pi w^2(r)\, r\, dr = 2\pi \bar{w}^2 a^2 \tag{B 4}$$

and the mass flux is

$$m = \int_0^\infty 2\pi w(r) r\, dr = 2\pi \bar{w} a^2. \tag{B 5}$$

We define the parameter

$$\bar{S} = \bar{w}k/\Omega,$$

where

$$\Omega = \Gamma_\infty / 2\pi a^2.$$

For the circulation distribution of (B 2) the parameter K, which determines the angular velocity of the filament, is

$$K = [-\ln(ka) - \ln(1{\cdot}65) - 0{\cdot}058 + \ln 2 - \gamma].$$

As shown by Saffman (1970) and others, $A = -0{\cdot}058$ for an exponentially decaying vortex; $\ln(1{\cdot}65)$ is a correction to account for the characteristic length $1{\cdot}65a$ in (B 3).

In terms of the parameter $\bar{S}$, the long wave stability quadratic (2.11) for the most critical mode $x_0 = iy_0$, becomes

$$\sigma^2 + 2\sigma\bar{S} + \bar{S}^2 - \tfrac{1}{2}(ka)^2 K - \sigma = 0, \tag{B 6}$$

the terms involving mass and momentum flux now being larger by a factor of 2. The roots of this quadratic are

$$\sigma = -\tfrac{1}{2}[2\bar{S} - 1] \pm \tfrac{1}{2}[(2\bar{S} - 1)^2 - 4\bar{S}^2 + 2(ka)^2 K]. \tag{B 7}$$

In this case, instability occurs for

$$\bar{S} > \tfrac{1}{4}(1 + 2(ka)^2 K). \tag{B 8}$$

Bergman presented contours of constant amplification rate λ_i as a function of ka and μ, μ defined as

$$\mu = \Gamma_\infty / a\bar{w}. \tag{B 9}$$

Because he uses a/w rather than $1/\Omega$ as his time scale, his amplification rate λ_i is equivalent to $\sigma_i \mu / 2\pi$, where σ_i is the imaginary part of σ, (B 7). The stability boundary $\sigma_i = 0$, however, corresponds to $\lambda_i = 0$. μ is equivalent to

$$\mu = 2\pi a^2 \Omega k / a\bar{w}k = 2\pi(ka)/\bar{S}. \tag{B 10}$$

Thus from (B 10) and (B 8) the long wave analysis predicts instability for

$$\mu < 8\pi(ka)/\{1 + 2(ka)^2 K\}. \tag{B 11}$$

This is presented in figure 4 and discussed in § 2.

REFERENCES

Batchelor, G. K. & Gill, A. E. 1962 Analysis of the stability of axisymmetric jets. *J. Fluid Mech.* **14**, 529.

Bergman, K. H. 1969 On the dynamic stability of convective atmospheric vortices. Ph.D. thesis, Department of Atmospheric Sciences, University of Washington.

Crow, S. C. 1970 Stability theory for a pair of trailing vortices. *AIAA Paper* 70–53. (To appear in *AIAA J.*)

Milne-Thompson, L. M. 1968 *Theoretical Hydrodynamics.* Macmillan.

MOORE, D. W. & SAFFMAN, P. B. 1971 Long wave oscillations of a vortex with axial flow. (To be published in *Studies in Applied Math.*)

SAFFMAN, P. B. 1970 The velocity of viscous vortex rings. *Proceedings of the Symposium on Aircraft Wake Turbulence*, Seattle, Washington.

THOMSON, W. 1910*a* Vibrations of a columnar vortex. *Mathematical and Physical Papers*, vol. IV. Cambridge University Press.

THOMSON, W. 1910*b* The translatory velocity of a circular vortex ring. *Mathematical and Physical Papers*, vol. IV. Cambridge University Press.

WIDNALL, S. E., BLISS, D. & ZALAY, A. 1970 Theoretical and experimental study of the stability of a vortex pair. *Proceedings of the Symposium on Aircraft Wake Turbulence*, Seattle, Washington.